

Received October 16, 2021, accepted October 26, 2021, date of publication November 1, 2021, date of current version November 9, 2021.

Digital Object Identifier 10.1109/ACCESS.2021.3124609

# Robust Motion Control of Nonlinear Quadrotor Model With Wind Disturbance Observer

SHEIKH IZZAL AZID<sup>1</sup>, (Member, IEEE), KRISHNEEL KUMAR<sup>2</sup>,  
MAURIZIO CIRRINCIONE<sup>1,3</sup>, (Senior Member, IEEE),  
AND ADRIANO FAGIOLINI<sup>4</sup>, (Member, IEEE)

<sup>1</sup>School of Information Technology, Engineering, Mathematics and Physics, The University of the South Pacific, Suva, Fiji

<sup>2</sup>Engineering and Complex Systems, University of Genoa, 16145 Genova, Italy

<sup>3</sup>Energy Department, The University of Technology of Belfort-Montbeliard, 90010 Belfort, France

<sup>4</sup>Mobile and Intelligent Robots@Panormous Laboratory (MIRPALab), Department of Engineering, University of Palermo, 90133 Palermo, Italy

Corresponding author: Sheikh Izzal Azid (sheikh.azid@usp.ac.fj)

This work was supported in part by the Joint Ph.D. Agreement between the University of the South Pacific and the University of Palermo, Palermo under the Project CORI-2017-D-D07-010083.

**ABSTRACT** This paper focuses on robust wind disturbance rejection for nonlinear quadrotor models. By leveraging on nonlinear unknown observer theory, it proposes a nonlinear dynamic filter that, using sensors already on-board the aircraft, can estimate in real-time wind gust signals in the three dimensions. The wind disturbance is then treated as input to the PD controller for a quick and robust flight pathway in presence of disturbances. With this scheme, the wind disturbance can be precisely estimated online and compensated in real-time. Hence, the quadrotor can successfully reach its desired attitude and position. To show the effective and desired performance of the method, simulation results are presented in Matlab/Simulink and ROS-enabled Gazebo platform.

**INDEX TERMS** Nonlinear unknown input observers, unknown wind gust estimation and compensation, quadrotor, PD control.

## I. INTRODUCTION

Unmanned Aerial Vehicles (UAVs) have drawn significant attention in many areas, ranging from the military, monitoring marine and agricultural sectors, disaster surveillance, to surveying and aerial robot manipulations. In all of such applications, UAVs are required to be robust and autonomous in any flight environment. Among them, quadrotor aircraft are multiple-input multiple-output (MIMO) systems, lightweight, highly nonlinear, and under-actuated. They rely on four fixed rotors and use variation in motor speeds for maneuvering. During their actual flights, quadrotors are always exposed to various disturbances and uncertainties, such as wind gusts, which results in difficulties in achieving robust performance and accurate flight paths.

Various linear and nonlinear control techniques have been developed for quadrotors, the most common of which are based on PID controllers. The work in [1] proposed a robust PID controller for trajectory tracking tasks as well as

maintaining stability for the nonlinear model of the quadrotor. Online self-tuning PID control has also shown good results where the PID controller parameters are dynamically tuned during the flight [2]. PD control and PD-Fuzzy method have been used to control the quadrotor which is a highly integrating system and has shown better robustness [3].

Moreover, nonlinear control methods are also used to achieve an advanced performance of the quadrotor. Some of the nonlinear techniques include feedback linearization [4], sliding mode [5] and backstepping [6]. They have demonstrated significant achievements in robust control of the nonlinear model of the quadrotor. The feedback linearization control algorithm transforms the nonlinear system model into an equivalent linear system through a change in variables. The linearization choice is between states and outputs [4]. However, the feedback linearization is highly sensitive to noise and is not as robust when compared to sliding mode controllers [7].

The control methods discussed above are used mainly to stabilize a quadrotor equipped with several sensors, inertial measurement units(IMU), and cameras which may lead to

The associate editor coordinating the review of this manuscript and approving it for publication was Shihong Ding<sup>1</sup>.

more weight, changes in the center of gravity, mass, and inertia of the quadrotor system. In general, all other control methods discussed will not be able to work efficiently if external disturbances are exposed to it as the disturbances have to be measured to ensure the aircraft's stability and resilience.

Furthermore, the stability and performance need to go along with the robustness of the overall system against external disturbances. To tackle this problem, different types of observers have been developed in the last three decades, including Extended Kalman Filters (EKF), Equivalent Input Disturbance (EID) estimator, Uncertainty and Disturbance Estimator (UDE), Generalized Proportional Integral Observer (GPIO), Extended State Observer (ESO) and Extended High Gain Observer (EHGO) [8], and Unknown Input Observers (UIO). Performance comparisons between these observers have been done in other domains and date back over some decades [9]–[16]. Based on these papers, EKF and ESO showed promising results; however, they are stochastic, still have issues in reconstructing the unknown inputs, and often require practical assumptions on the disturbance that are not satisfied in reality. Indeed, the ESO/GESO method requires that the uncertainties act via the same channel as that of the control input [17]. Moreover, a UIO-based approach performs in general at least as much as the corresponding one with the EKF and ESO methods, but in many other situations, it combines easy design with superior performance.

Robustness is a major concern for a quadrotor aircraft in the case of unknown disturbances, such as the wind, since the system may become unstable and, therefore, will face challenges in controlling and stabilizing in the presence of wind. Kalman filters, including EKF, have been applied to estimate the disturbances [18], [19], however, it is a stochastic approach. The work in [20] proposed UAV state, external wind, and parameter estimation in windy conditions using unscented Kalman filter based on IMU and ground velocity measurements. However, these methods require numerous assumptions for noise.

Over the years, research in the design of observers has accumulated through literature to obtain high accuracy, low cost, and good prediction performances of systems. Luenberger observer evaluates a given set of linear functions of the state observers to extract the unknown input of the system using a geometric approach [12]. The inversion algorithm of Silverman has been used in [21] to show the dynamic portion of the inverse system which gives a partial state observer of the system, having completely unknown inputs. A reduced-order state observer for discrete-time linear system models with unknown inputs, also known as UIO, has been developed in [22]. This approach provides a characterization of observers with delay, which eases the establishment of necessary conditions for the existence of UIO with zero delays. By introducing a delay, the observer has the potential to be used in a variety of systems and applications such as feedback control, fault diagnosis and system identification [23].

Later on, the research has shifted from linear to nonlinear observers. Earlier class of nonlinear Lipschitz system has been studied [24], where the observer design relies on the linear setting by imposing certain conditions on the nonlinearities. This approach inherits drawbacks from the observer convergence conditions that are difficult to be satisfied for large Lipschitz constants [25]. The problem is solved later with the use of a Lyapunov function to guarantee asymptotic stability [26]. The increasing convergence rate showed good robustness. Moreover [27] extended the observer design using differential mean value theorem on the basics of Lyapunov approach and linear matrix inequality conditions and also decoupled the unknown inputs.

One of the most challenging tasks for a UAV is to achieve every control objective in terms of trajectory in spite of the presence of external disturbances, such as sudden wind gusts. Indeed, the dynamical model of a UAV, including that of a quadrotor, is highly nonlinear and moreover has two degrees of under actuation, since it has only four inputs and six outputs (the linear and angular positions). In this respect the control action is very hard and it becomes very challenging in the presence of wind gusts. Due to the existence of these external disturbances, much effort has been devoted to the design of a robust controller for the quadrotors.

Hence, robust control of quadrotors has been an interesting area of research. PID and intelligent active force control is proposed by [28] to improve disturbance rejection capability and robust trajectory. On the other hand, [29] proposed backstepping and sliding mode control in a double loop structure for effective trajectory tracking for the desired position of quadrotor model with disturbances. The work in [30], [31] have proposed high order sliding mode control to suppress the chattering when compared to traditional method while preserving robustness properties. These methods generally aim to retain insensitivity to model uncertainties and external disturbances in different ways, but do not estimate the disturbances to compensate. As a result, they may be slow in reacting to abrupt external disturbances. Visual-based robust position control of a quadrotor using sensors including IMU ultrasonic sensor and vision sensor is addressed by [32]. The design includes compensators to enhance robustness against disturbances. Furthermore, research work on observers recently has been applied to the UAVs for various applications. [33] used nonlinear observer for simultaneous localization and mapping, hence reducing error asymptotically. The work in [34] proposed  $H_\infty$  observers to address actuator faults and state estimation in presence of disturbances of quadrotors. Moreover, [35] utilizes a fuzzy structure to approximate the model unknown parts based on the composite surfaces of the under-actuated MIMO systems for coping with plant uncertainties and, specifically, with actuator deadzones. Disturbance observers have been used for aggressive maneuvering for attitude control, velocity tracking, and flight control of quadrotors [36]. In general, robust control has been divided into two categories: suppressing disturbances via feedback control such as second order

sliding mode control [28]–[31] or cancelling disturbances by feedforward control [32]–[36]. In the latter, the reverse of disturbance signal is feed forwarded so that the robustness of a system is intuitively achieved by cancelling disturbances, the main drawback of this robust control technique is that disturbances are unknown or unmeasurable.

*Contribution:* With this respect, the paper presents a complementary yet innovative wind disturbance rejection approach, where wind disturbance is promptly estimated online by a Nonlinear Unknown Input Observer (NUIO). The appealing features of the developed scheme are its simplicity, low computation cost, ability to obtain a fast response to wind gusts, and implementability on virtually all aircraft systems, as a stand-alone solution or an extension plugin for existing controllers. More specifically:

- 1) the low computation demand is inherited by the simplicity of the NUIO, which requires no additional sensors and that robustly estimates the overall effects of wind disturbance and other model uncertainty;
- 2) The promptness and efficacy of the estimator, along with the position recovery scheme, are shown to outperform existing solutions based on EKF, GESO, model predictive control, and robust control;
- 3) In this respect, it should also be noted that traditional robust control involves complex controllers and is unable to react fast enough in the presence of strong disturbances [8], [37], [38] or may require the application of a signal that is too conservative or even unfeasible; in contrast, the present approach compensates for the exact amount of disturbance which is estimated online;
- 4) Finally, by being independent of the type of control law used to determine the rotor speeds of the aircraft, the developed scheme can provide existing controllers with the additional capacity to better deal with disturbances. This fact is shown in the paper, both in simulation and via experiments, on a platform using an open-source, the standard Ardupilot controller, which communicates with the estimator via a ROS middleware layer.

## II. QUADROTOR MATHEMATICAL MODEL

A quadrotor aircraft consists of a planar cross-shaped rigid chassis, actuated by four independent rotors which are mounted at the tips of the arms of the chassis itself (Fig. 1).

The aircraft pose information is measured via sensors: the position  $(x, y, z)$  of its center of mass is measured via GPS sensors which provide data in the inertial Earth frame  $F_0$ , while the orientation  $(\phi, \theta, \psi)$  is obtained from Inertial Measurement Units (IMU) in a body frame  $F_B$ . The state vector of a quadrotor vehicle consists of the following 12 variables: the positions  $(x, y, z, \phi, \theta, \psi)$  and velocities  $(u, v, w, p, q, r)$ . As shown in Fig. 1, the four rotors apply a force orthogonal to the rotation plane of their blades which are aligned with the positive  $z$ -axis of the body frame  $F_B$  and proportional to the rotation speed square, i.e.  $F_i = K_F \omega_i^2$ , where  $i$  is the  $i$ -th rotor. Each force  $F_i$  generates a torque along the

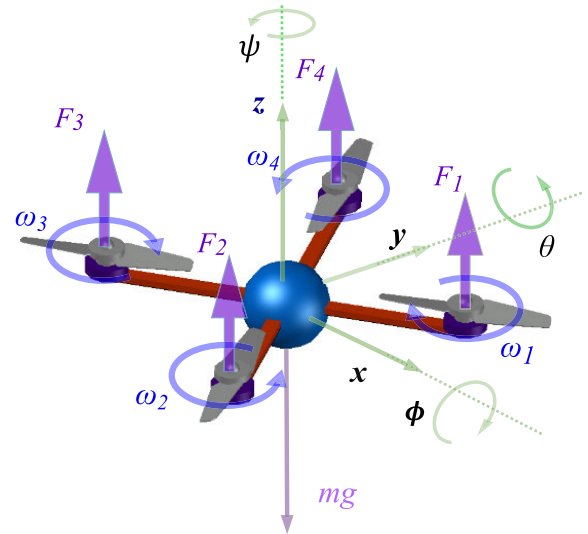


FIGURE 1. Quadrotor mechanical structure, model and reference frames.

orthogonal axis which is represented by the opposite arm of the aircraft chassis, being  $lK_F \omega_i^2$ , where  $l$  is the arm length. Each rotor produces a torque, due to air drag, that is opposite to its rotation and whose absolute value is proportional to its rotation speed, that is,  $K_M \omega_i^2$ . Therefore, the overall thrust  $F_z$  and the components of the torque vector  $(\tau_\phi, \tau_\theta, \tau_\psi)$  are linearly coupled with the squares of rotor speeds. All such quantities are grouped in the state and input vectors:

$$\xi = (x, y, z, \phi, \theta, \psi, u, v, w, p, q, r)^T, \quad (1)$$

$$U = \begin{pmatrix} F_z \\ \tau_\phi \\ \tau_\theta \\ \tau_\psi \end{pmatrix} = \begin{pmatrix} K_F(\omega_1^2 + \omega_2^2 + \omega_3^2 + \omega_4^2) \\ lK_F(\omega_2^2 - \omega_4^2) \\ lK_F(\omega_1^2 - \omega_3^2) \\ K_M(\omega_1^2 - \omega_2^2 + \omega_3^2 - \omega_4^2) \end{pmatrix}. \quad (2)$$

Furthermore, among available possibilities, the ZXY convention has been chosen to align the axes of  $F_0$  to those of  $F_B$ . The aircraft orientation is obtained by rotating first  $F_0$  about the  $z$ -axis of  $\psi$  (yaw) radians, the about the new  $x$ -axis of  $\phi$  (roll) radians, and finally about the resulting  $y$ -axis of  $\theta$  (pitch) radians. Accordingly, considering the elementary rotations

$$R_x(\phi) = \begin{pmatrix} 1 & 0 & 0 \\ 0 & c_\phi & s_\phi \\ 0 & -s_\phi & c_\phi \end{pmatrix}, \quad R_y(\theta) = \begin{pmatrix} c_\theta & 0 & -s_\theta \\ 0 & 1 & 0 \\ s_\theta & 0 & c_\theta \end{pmatrix},$$

$$R_z(\psi) = \begin{pmatrix} c_\psi & s_\psi & 0 \\ -s_\psi & c_\psi & 0 \\ 0 & 0 & 1 \end{pmatrix}, \quad (3)$$

where  $s_* = \sin(*)$  and  $c_* = \cos(*)$ , the complete rotation converting body-frame coordinates into inertial ones is

$$R_{zxy} = (R_z(\psi)R_x(\phi)R_y(\theta))^T$$

$$= \begin{pmatrix} c_\theta c_\psi - s_\phi s_\theta s_\psi & -c_\phi s_\psi & s_\theta c_\psi + s_\phi c_\theta s_\psi \\ c_\theta s_\psi + s_\phi s_\theta c_\psi & c_\phi c_\psi & s_\theta s_\psi - s_\phi c_\theta c_\psi \\ -c_\phi s_\theta & s_\theta & c_\phi c_\theta \end{pmatrix}. \quad (4)$$

The forces acting on the quadrotor center of mass are the total thrust  $F$  applied by the four rotors (always aligned with the positive  $z$ -axis of the  $F_B$ ), the gravity force (which is oriented along the negative direction of the  $z$ -axis of  $F_0$ ), and the wind gusts,  $W = (W_x, W_y, W_z)^T$  (whose components are assumed to be expressed in  $F_0$  by convention). Indicating with  $m$  the aircraft mass and  $g$  the gravity acceleration, Newton's equations for the translational motion of the center of mass read:

$$m \begin{pmatrix} \ddot{x} \\ \ddot{y} \\ \ddot{z} \end{pmatrix} = -m \begin{pmatrix} 0 \\ 0 \\ g \end{pmatrix} + R_{zxy} \begin{pmatrix} 0 \\ 0 \\ F \end{pmatrix} + W, \quad (5)$$

which can be expanded as

$$\begin{pmatrix} m\ddot{x} \\ m\ddot{y} \\ m\ddot{z} \end{pmatrix} = \begin{pmatrix} (s_\theta c_\psi + s_\phi c_\theta s_\psi)F + W_x \\ (s_\theta s_\psi - s_\phi c_\theta c_\psi)F + W_y \\ (c_\phi c_\theta)F - mg + W_z \end{pmatrix}. \quad (6)$$

Furthermore, the angular velocity vector  $(p, q, r)^T$  of the aircraft in body frame  $F_B$  can be related to the Euler angles through a dynamic relation which reads, for the ZXY convention, as

$$\begin{pmatrix} p \\ q \\ r \end{pmatrix} = \begin{pmatrix} 0 \\ \dot{\theta} \\ 0 \end{pmatrix} + R_y(\theta) \begin{pmatrix} \dot{\phi} \\ 0 \\ 0 \end{pmatrix} + R_y(\theta)R_x(\phi) \begin{pmatrix} 0 \\ 0 \\ \dot{\psi} \end{pmatrix},$$

which can be compactly written as

$$\begin{pmatrix} p \\ q \\ r \end{pmatrix} = \begin{pmatrix} c_\theta & 0 & -s_\theta \\ 0 & 1 & 0 \\ s_\theta & 0 & c_\theta \end{pmatrix} \begin{pmatrix} \dot{\phi} \\ \dot{\theta} \\ \dot{\psi} \end{pmatrix}. \quad (7)$$

Due to the lean and trim structure of the quadrotor, it is assumed that the wind momentum is negligible, thereby implying that the vector  $T = (\tau_\phi, \tau_\theta, \tau_\psi)^T$  acting on the aircraft itself is composed of the torques applied by the spinning of the rotors. Since  $F_B$  is aligned with the principal inertia axes of the aircraft, Euler's equations for the angular motion read

$$T = I \begin{pmatrix} \dot{p} \\ \dot{q} \\ \dot{r} \end{pmatrix} + \begin{pmatrix} 0 & -r & q \\ r & 0 & -p \\ -q & p & 0 \end{pmatrix} I \begin{pmatrix} p \\ q \\ r \end{pmatrix}, \quad (8)$$

where  $I = \text{diag}(I_{xx}, I_{yy}, I_{zz})$  is the inertia matrix around the axes of  $F_B$ . Direct computation of (8) leads to

$$\begin{pmatrix} I_{xx} \dot{p} \\ I_{yy} \dot{q} \\ I_{zz} \dot{r} \end{pmatrix} = \begin{pmatrix} \tau_\phi - (I_{zz} - I_{yy})qr \\ \tau_\theta - (I_{xx} - I_{zz})pr \\ \tau_\psi - (I_{yy} - I_{xx})pq \end{pmatrix}. \quad (9)$$

Summing up, Eq. (6), (7), and (9) are one possible nonlinear dynamic model of a quadrotor aircraft. In state space, such a model reads

$$\begin{aligned} \dot{x} &= u, \\ \dot{y} &= v, \\ \dot{z} &= w, \\ \dot{\phi} &= p c_\theta + r s_\theta, \end{aligned}$$

$$\begin{aligned} \dot{\theta} &= \frac{s_\phi}{c_\phi} s_\theta p + q - \frac{s_\phi}{c_\phi} c_\theta r \\ \dot{\psi} &= -\frac{s_\theta}{c_\phi} p + \frac{c_\theta}{c_\phi} r, \\ \dot{u} &= (s_\theta c_\psi + s_\phi c_\theta s_\psi) \frac{F}{m} + \frac{W_x}{m}, \\ \dot{v} &= (s_\theta c_\psi - s_\phi c_\theta s_\psi) \frac{F}{m} + \frac{W_y}{m}, \\ \dot{w} &= c_\phi c_\theta \frac{F}{m} - g + \frac{W_z}{m} \\ \dot{p} &= -\frac{I_{zz} - I_{yy}}{I_{xx}} q r + \frac{\tau_\phi}{I_{xx}}, \\ \dot{q} &= -\frac{I_{xx} - I_{zz}}{I_{yy}} p r + \frac{\tau_\theta}{I_{yy}}, \\ \dot{r} &= -\frac{I_{yy} - I_{zz}}{I_{zz}} p q + \frac{\tau_\psi}{I_{zz}}. \end{aligned} \quad (10)$$

### III. NONLINEAR OBSERVERS FOR QUADROTOR MODELS WITH UNKNOWN INPUT DISTURBANCE

Consider a nonlinear model affected by an unknown input disturbance  $w$  and described by the discrete-time form

$$\begin{aligned} \xi(k+1) &= A \xi(k) + f(\xi(k)) + g(u(k), \eta(k)) + D w(k), \\ \eta(k) &= C \xi(k), \end{aligned} \quad (11)$$

where  $\xi \in \mathbb{R}^n$  is the state vector,  $u \in \mathbb{R}^m$  is a known input vector,  $w \in \mathbb{R}^k$  is the vector of the unknown input,  $\eta \in \mathbb{R}^p$  is an output vector. Moreover,  $A$  is the state matrix,  $C$  is the output matrix,  $D$  is the disturbance matrix of suitable sizes, and  $g : \mathbb{R}^{m+p} \rightarrow \mathbb{R}^n$  and  $f : \mathbb{R}^n \rightarrow \mathbb{R}^n$  are nonlinear functions. Then, the nonlinear quadrotor model (10) in Sec. II can be written as in (11) by defining

$$A = \begin{pmatrix} 0_{3 \times 3} & I_{3 \times 3} & 0_{3 \times 3} & 0_{3 \times 3} \\ 0_{3 \times 3} & 0_{3 \times 3} & 0_{3 \times 3} & 0_{3 \times 3} \\ 0_{3 \times 3} & 0_{3 \times 3} & 0_{3 \times 3} & Q \\ 0_{3 \times 3} & 0_{3 \times 3} & 0_{3 \times 3} & 0_{3 \times 3} \end{pmatrix}, \text{ with } Q = \begin{pmatrix} 0 & 0 & 0 \\ 0 & 1 & 0 \\ 0 & 0 & 0 \end{pmatrix} \quad (12)$$

and

$$\begin{aligned} f(\xi) &= \begin{pmatrix} 0_{5 \times 1} \\ -g \\ c_\theta p + s_\theta r \\ \frac{s_\phi}{c_\phi} s_\theta p + \frac{s_\phi}{c_\phi} c_\theta r \\ \frac{s_\theta}{c_\phi} p + \frac{c_\theta}{c_\phi} r \\ -\frac{I_{zz} - I_{yy}}{I_{xx}} q r \\ -\frac{I_{xx} - I_{zz}}{I_{yy}} p r \\ -\frac{I_{yy} - I_{xx}}{I_{zz}} p q \end{pmatrix}, \\ g(u, \eta) &= \begin{pmatrix} 0_{3 \times 1} & 0_{3 \times 3} \\ (s_\theta c_\psi + s_\phi c_\theta s_\psi) \frac{F}{m} & 0_{3 \times 3} \\ (s_\theta c_\psi - s_\phi c_\theta s_\psi) \frac{F}{m} & 0_{3 \times 3} \\ c_\phi c_\theta & \\ 0_{3 \times 1} & 0_{3 \times 3} \\ 0_{3 \times 1} & \Phi \end{pmatrix}, \end{aligned} \quad (13)$$

where  $\Phi = \text{diag}(\tau_\phi/I_{zz}, \tau_\theta/I_{yy}, \tau_\psi/I_{zz})$ , and the unknown wind gust matrix is  $D = (0_{3 \times 3}, 0_{3 \times 3}, I_{3 \times 3}/m, 0_{3 \times 3})^T$ .

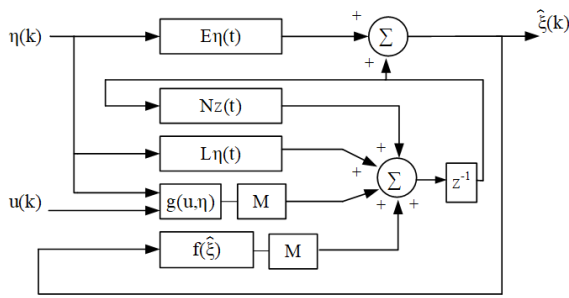


FIGURE 2. Depiction of the proposed Nonlinear Unknown Input Observer.

Assuming  $D$  be full-column rank ensures the possibility to reconstruct the unknown input  $w$  once the system states have been recovered. Moreover, to ensure the full observability of the system state the output vector has been chosen as  $\eta = (x, y, z, \phi, \theta, \psi, u, v, w)^T$ . The below described estimation process, based on the NUIO, is depicted in Fig. 2.

Referring to the scheme proposed in [27], the state estimate  $\hat{\xi}(k) = z(k) - E \eta(k)$  is defined, where  $\eta$  is the system output and  $\zeta$  is an observer variable whose dynamics reads:

$$z(k + 1) = N z(k) + L \eta(k) + M f(\hat{\xi}(k)) + M g(u(k), \eta(k)), \quad (15)$$

where  $N, L, M$  and  $E$  are unknown matrices of appropriate dimensions which must be determined so that  $\hat{\xi}(k)$  asymptotically converges to  $\xi(k)$ . More precisely,  $N, L$  and  $M$  can be chosen as

$$\begin{aligned} N &= MA - LC, \\ L &= K(I_p + EC) - MAE, \\ M &= I_n + EC, \end{aligned} \quad (16)$$

and  $E$  and  $K$  are obtained via the observer design. By introducing the estimation error,

$$e(k) = \xi(k) - \hat{\xi}(k) = \xi(k) - z(k) + E \eta(k) \quad (17)$$

its error dynamics reads

$$e(k + 1) = (I_n + EC) \xi(k + 1) - z(k + 1). \quad (18)$$

Using (11) and (15) the error dynamics can be rewritten as

$$e(k + 1) = N e(k) + (MA - LC - NM) \xi(k) + M (f(\xi(k)) - f(\hat{\xi}(k))) + MD w(k).$$

Using (16),  $MA - LC - NM$  is equal to zero, and, consequently, the error dynamics reduces to

$$e(k + 1) = N e(k) + M (f(\xi(k)) - f(\hat{\xi}(k))) + MD w(k). \quad (19)$$

It is necessary for the error dynamics to converge to zero, hence, by using differential mean value theorem

$$M (f(\xi(k)) - f(\hat{\xi}(k))) = M \mathcal{J} c(k), \quad (20)$$

for some  $c \in (\xi(k), \hat{\xi}(k))$  and where the Jacobian matrix  $\mathcal{J}$  has been developed for the hovering condition of the quadrotor with  $\phi, \theta \approx 0$ . In this way, the quadrotor has 4 outputs and 4 control inputs, the system is fully manageable, and the pair  $A(\alpha)$  and  $C$  are observable. Therefore,

$$\mathcal{J}_f = \begin{pmatrix} 0_{6 \times 12} \\ 0_{3 \times 6} & J_{33} & (I_{3 \times 3} - Q) \\ 0_{3 \times 9} & & J_{44} \end{pmatrix} \quad (21)$$

where

$$J_{33} = \begin{pmatrix} 0 & r & 0 \\ -r & 0 & 0 \\ 0 & -p & 0 \end{pmatrix}, \quad J_{44} = \begin{pmatrix} 0 & r\Gamma & q\Gamma \\ -r\Delta & 0 & -p\Delta \\ q\Lambda & p\Lambda & 0 \end{pmatrix}$$

and  $\Gamma = \frac{(J_{yy} - I_{zz})}{I_{xx}}, \Delta = \frac{(I_{xx} - I_{zz})}{I_{yy}}, \Lambda = \frac{(I_{xx} - I_{yy})}{I_{zz}}$ . Hence,

$$A(\alpha) = A + \mathcal{J}_f(\alpha) = \begin{pmatrix} 0_{3 \times 3} & I_{3 \times 3} & 0_{3 \times 3} & 0_{3 \times 3} \\ 0_{3 \times 3} & 0_{3 \times 3} & 0_{3 \times 3} & 0_{3 \times 3} \\ 0_{3 \times 3} & 0_{3 \times 3} & J_{33} & I_{3 \times 3} \\ 0_{3 \times 3} & 0_{3 \times 3} & 0_{3 \times 3} & J_{44} \end{pmatrix}, \quad (22)$$

where  $\alpha$  is the set of all vertices  $\{a_{ij}\}$  and  $i, j = 1, \dots, n$ .

Moreover, as per the theorem outlined by [27], if there exist  $E, K$  and a positive defined matrix  $P$ , such that the matrix  $\begin{pmatrix} -P & X \\ X & P \end{pmatrix}$ , where  $X = PA(\alpha) + PUC A(\alpha) + P_s VCA(\alpha) - KC$ , is negative definite, then the state estimation error asymptotically converges, i.e.  $e(k) \rightarrow 0$  as  $k \rightarrow \infty$ . Then, the unknown input decoupled to  $(EC + I_n)D = 0$ , which implies  $EC D = -D$  and consequently  $MD = 0$ . The error dynamics then becomes

$$e(k + 1) = N e(k) + M \mathcal{J}(k) e(k).$$

Moreover, with the corresponding output matrix  $C = (I_{9 \times 9}, 0_{9 \times 3})$  and unknown input matrix  $D$ , to have appropriate solution for  $E$  the following condition has to be satisfied:

$$\text{rank} \begin{pmatrix} CD \\ D \end{pmatrix} = \text{rank}(CD) \quad (23)$$

From (23), all solutions of  $E$  using generalised inverse are:  $E = -D(CD)^\dagger + S(I_p - (CD)(CD)^\dagger)$ . Then, it holds

$$U = -D(CD)^\dagger = \begin{pmatrix} 0_{3 \times 3} & 0_{3 \times 3} & 0_{3 \times 3} & 0_{3 \times 3} \\ 0_{3 \times 3} & -I_{3 \times 3} & 0_{3 \times 3} & 0_{3 \times 3} \\ 0_{6 \times 3} & 0_{6 \times 3} & 0_{6 \times 3} & 0_{6 \times 3} \end{pmatrix},$$

$$V = I_p - (CD)(CD)^\dagger = \begin{pmatrix} I_{3 \times 3} & 0_{3 \times 6} & 0_{3 \times 3} \\ 0_{6 \times 3} & 0_{6 \times 6} & 0_{3 \times 3} \\ 0_{3 \times 3} & 0_{3 \times 6} & I_{3 \times 3} \end{pmatrix}.$$

Moreover, considering the Lyapunov candidate  $V(k) = e^T(k) P e(k)$ , the following forward difference is to be considered:

$$\begin{aligned} \Delta V &= V(k + 1) - V(k) \\ &= e^T(k) \left( (MA \mathcal{J}(k) - KC)^T P \right. \\ &\quad \left. \times (MA \mathcal{J}(k) - KC) - P \right) e(k). \end{aligned}$$

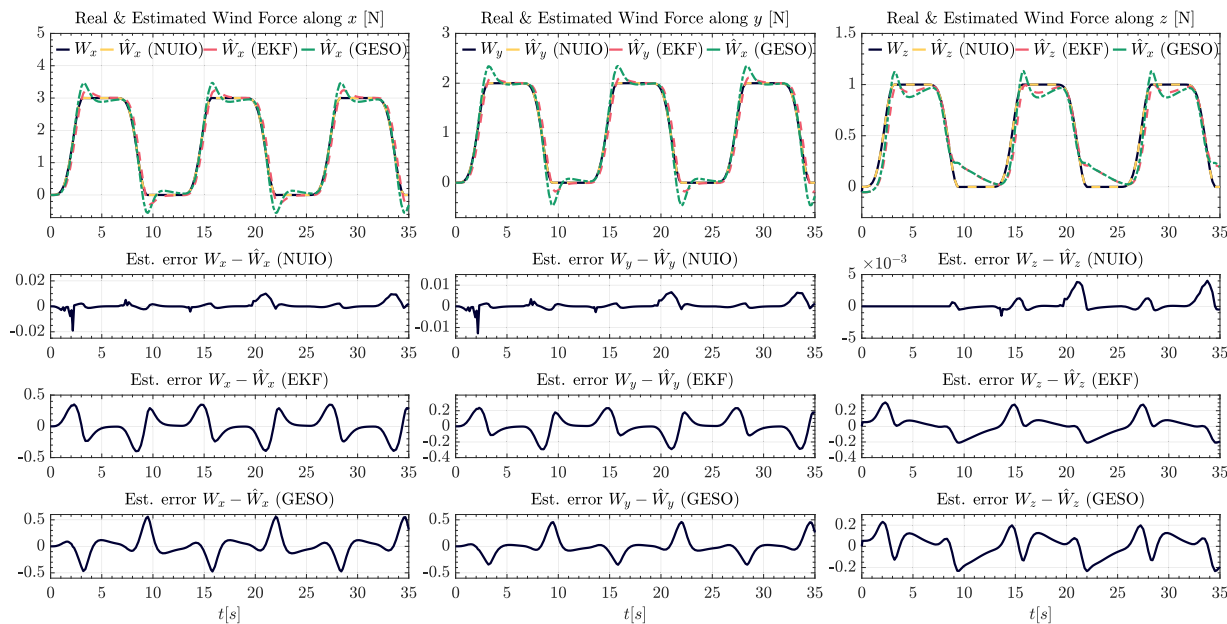


**FIGURE 3.** Estimated versus actual wind gusts for the time varying wind gust model. The NUIO error is at least 25 times smaller than EKF and GESO.

The above equation can be solved using the Linear Matrix Inequality (LMI) technique in Matlab. For the error to be convergent, it is required for  $\Delta V < 0$ . To begin with, by using the above expression  $\Delta V = e^T(k)[X^T P^{-1} X - P]e(k)$ , where  $X = PA(\alpha) + PUC A(\alpha) + P_s VCA(\alpha) - KC$ ,  $P_s = PS$  and  $P_k = 0$ . This further implies  $X^T P^{-1} X - P < 0$ . Then, by using LMI with the condition  $P > 0$ , the solutions for  $P, P_s, P_k$  can be found. Moreover, the matrix inequalities  $PA(\alpha) + PUC A(\alpha) + P_s VCA(\alpha) - KC$  and  $P < 0$  are verified for all  $\alpha_{ij}$ , with  $i, j = 1, \dots, n$ . If so the sought condition is met, the eigenvalues are negative, and the estimation error converges. Furthermore, matrices  $N = MA - KC$  and  $L = K(I_p + CE) - MAE$  are computed, since they are required by the observer design as expressed in 11. Finally, the unknown input vector  $w$  is reconstructed as:

$$w(k) = D^\dagger \left( \hat{\xi}_{k+1} - A_d \hat{\xi}_k - f(\hat{\xi}_k) - g(u_k, \eta_k) \right) \quad (24)$$

with  $D^\dagger = (D^T D)^{-1} D^T$ .

It is notable to compare Extended Kalman Filters (EKF) and Generalised Extended State Observers (GESO) to Non-linear Unknown Input Observer (NUIO). In general, a NUIO has a deterministic approach and performs superior when compared to EKF and GESO which has a stochastic approach. Fig. 3 shows the estimated time-varying wind gust force with peak amplitudes of  $W_x = 3$  N,  $W_y = 2$  N, and  $W_z = 1$  N, acting on the nonlinear model of the quadrotor aircraft. The yellow line shows the estimated wind gusts extracted from the NUIO, while the dotted line shows the estimation by an EKF (red) and GESO (green). The references are given in black. The NUIO estimation is so error is so small

that its graph sits on top of the reference plot. The comparison reveals that the NUIO is superior in estimating the unknown wind gust and provides the fastest response among the three types of estimators; when compared to the EKF and GESO, also it does not have high peaks. Moreover, for the EKF, numerous process noise and measurement noise values were simulated from which a process noise and measurement noise were selected to give the best performance. Similarly, the GESO was tuned to give the best performance. Fig. 3 shows that amplitude of the estimation error achieved by the NUIO is about 25 times smaller than that of the EKF and 50 times smaller in the case of the GESO. Similar trend occurs also as for what it concerns the state estimation which is shown in Fig. 4.

#### IV. WIND GUST COMPENSATION

The proposed estimation and control scheme ensuring the achievement of accurate and robust path tracking even with wind disturbance is illustrated in Fig. 5. According to it, a NUIO estimates the unknown wind gusts in real-time, as described in the previous section, and provides this information to a PD controller to compensate for it and to regulate the nonlinear model of the quadrotor. More specifically, having denoted with  $(x_d, y_d, z_d, \psi_d)$  the desired pose for the aircraft, an Attitude Control is used for the orientation in  $\phi, \theta, \psi$ , while a Position Control is used for positioning the quadrotor along the axes  $x, y$ , and  $z$ , by employing the information of the estimated wind gusts  $\hat{W}_x, \hat{W}_y, \hat{W}_z$  obtained via the NUIO. For the results obtained, the quadrotor is in a hovering state, which implies that  $\phi, \theta \approx 0$  for the system to be fully controllable, which are 4 inputs and 4 outputs. For the NUIO, 9 out of 12 states are measurable for simulation,

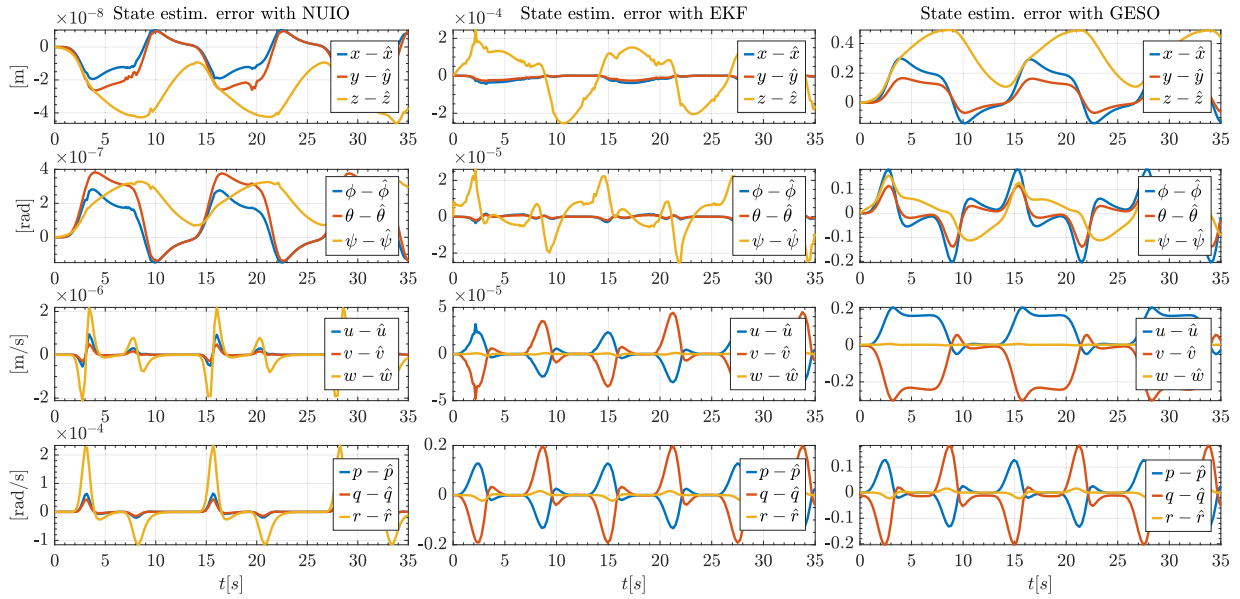


**FIGURE 4.** Plots of state estimation errors of the proposed NUIO (left) vs an EKF (middle) and a GESO (right). The estimator error obtained via the NUIO is at least  $10^2$  and  $10^4$  times smaller than those of the EKF and GESO.

that are  $x, y, z, \phi, \theta, \psi, u, v, w$ . These are used by the NUIO to estimate the 3 remaining states as well as the 3 unknown wind gust components. The details of the controller are described below.

**A. ESTIMATED WIND FEEDBACK WITH PD CONTROL**

The aim is to achieve accurate path tracking by the controlled quadrotor even in the presence of wind gust vectors  $(W_x, W_y, W_z)^T$  affecting the aircraft position. The PD controller is based on the approximated linear dynamic model of the quadrotor aircraft in hovering condition when  $\phi, \theta \approx 0$ . Let such nominal conditions be described by  $(x_d, y_d, z_d, \psi_d)$  and the nominal force for hovering,  $\bar{f} = g$ . Hence, the tracking error variables be  $\delta x = x - x_d, \delta y = y - y_d, \delta z = z - z_d$ , and  $\delta \psi = \psi - \psi_d$ . Moreover, the input variation variables are  $\delta f = f - g, \delta \phi = \phi - \phi_C$ , and  $\delta \theta = \theta - \theta_C$ . The linearized model (6), describing the quadcopter position, becomes

$$\begin{pmatrix} m\ddot{x} \\ m\ddot{y} \\ m\ddot{z} \end{pmatrix} = \begin{pmatrix} g s_{\psi_d} \delta \phi + g c_{\psi_d} \delta \theta + W_x \\ -g c_{\psi_d} \delta \phi + g s_{\psi_d} \delta \theta + W_y \\ \delta f + W_z \end{pmatrix}, \quad (25)$$

where  $\delta f \approx \frac{8 K_F \omega_0}{m} (\delta \omega_1 + \delta \omega_2 + \delta \omega_3 + \delta \omega_4)$ . To ensure the asymptotic convergence of the quadrotor center of mass to the desired position, the dynamic model in (25) is forced to follow the dynamics

$$\begin{pmatrix} \ddot{x} \\ \ddot{y} \\ \ddot{z} \end{pmatrix} = - \begin{pmatrix} k_x^v \dot{x} + k_x^p \delta x \\ k_y^v \dot{y} + k_y^p \delta y \\ k_z^v \dot{z} + k_z^p \delta z \end{pmatrix}. \quad (26)$$

By comparing (25) and (26), the relations for the rotor speed variations and the commanded roll and pitch,  $\phi_C$  and

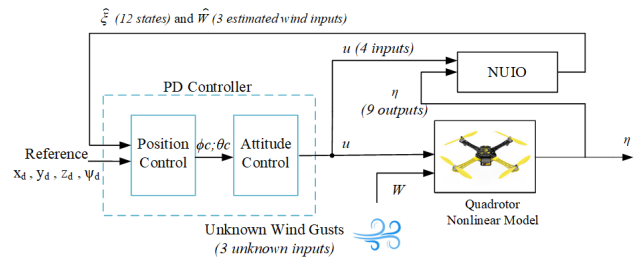


**FIGURE 5.** System architecture. The aircraft pose information is used within the NUIO which provides accurate estimates of all system states and wind disturbance; such an information is then used in the attitude and position controllers.

$\theta_C$  (see Eq. (31)) are obtained as follows:

$$\begin{pmatrix} \phi_C \\ \theta_C \\ f \end{pmatrix} = \begin{pmatrix} -\frac{R(\psi_d)}{g} \left( k_x^v \dot{x} + k_x^p (x - x_d) - \frac{W_x}{m} \right) \\ -\frac{R(\psi_d)}{g} \left( k_y^v \dot{y} + k_y^p (y - y_d) - \frac{W_y}{m} \right) \\ \frac{K_F}{m} \sum_{i=1}^4 \omega_i^2 + 2\sqrt{\frac{K_F}{m}} \delta \omega_z + \frac{W_z}{m} \end{pmatrix} \quad (27)$$

where

$$R(\psi_d) = \begin{pmatrix} s_{\psi_d} & -c_{\psi_d} \\ c_{\psi_d} & s_{\psi_d} \end{pmatrix},$$

$$\delta \omega_z = -k_z^v \dot{z} - k_z^p (x - z_d) + \frac{W_z}{m}.$$

Moving now on to the aircraft attitude control, from (10), the angular accelerations can be rewritten as

$$\begin{pmatrix} I_{xx} \dot{p} \\ I_{yy} \dot{q} \\ I_{zz} \dot{r} \end{pmatrix} = \begin{pmatrix} l K_F (\omega_2^2 - \omega_1^2) \\ l K_F (\omega_3^2 - \omega_1^2) \\ K_M (\omega_1^2 - \omega_2^2 + \omega_3^2 - \omega_4^2) \end{pmatrix} - \begin{pmatrix} I_1 q r \\ I_2 p r \\ I_3 p q \end{pmatrix} \quad (28)$$

with  $I_1 = I_{xx} - I_{yy}, I_2 = I_{xx} - I_{zz}$ , and  $I_3 = I_{zz} - I_{yy}$ .

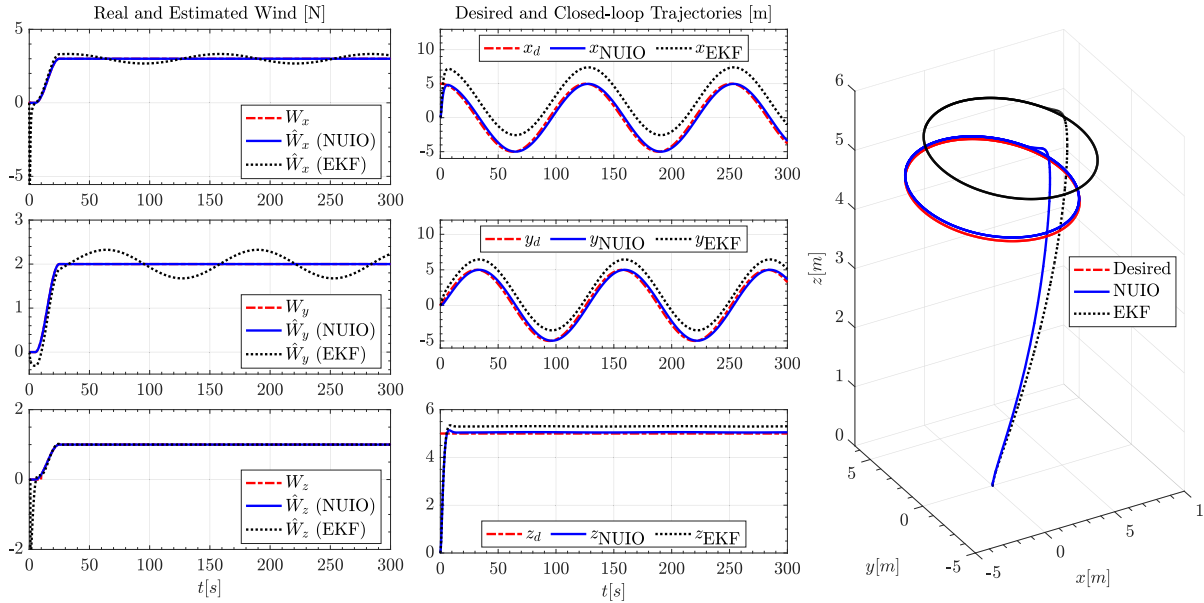


**FIGURE 6. Scenario #1 (Matlab simulation) - Wind estimation (left) with military grade wind gusts, desired and closed-loop trajectories with NUIO and EKF-based schemes (middle), tridimensional plot of the desired and closed-loop trajectories (right). The NUIO-based approach is very accurate and prompt, thereby allowing a superior control of the aircraft position.**

At hovering  $\phi, \theta \approx 0$ , thus it holds  $\dot{\phi} \approx p, \dot{\theta} \approx q$ , and  $\dot{\psi} \approx r$ . The attitude dynamics simplifies to

$$\begin{pmatrix} \ddot{\phi} \\ \ddot{\theta} \\ \ddot{\psi} \end{pmatrix} = \begin{pmatrix} \frac{IK_F}{I_{xx}}(\omega_2^2 - \omega_4^2) - \frac{I_{zz} - I_{yy}}{I_{xx}}\dot{\theta}\dot{\psi} \\ \frac{IK_F}{I_{yy}}(\omega_3^2 - \omega_1^2) - \frac{I_{xx} - I_{zz}}{I_{yy}}\dot{\phi}\dot{\psi} \\ \frac{K_M}{I_{zz}}(\omega_1^2 - \omega_2^2 + \omega_3^2 - \omega_4^2) - \frac{I_{xx} - I_{yy}}{I_{zz}}\dot{\phi}\dot{\theta} \end{pmatrix} \quad (29)$$

After linearizing (29) around the hovering conditions,  $\omega_i \approx \omega_0 = \sqrt{\frac{mg}{4K_F}}$ . Having denoted  $\delta\psi = \psi - \psi_d$  and  $\delta\omega_i = \omega_i - \omega_0$ , the linearized model reads

$$\begin{pmatrix} \ddot{\delta\phi} \\ \ddot{\delta\theta} \\ \ddot{\delta\psi} \end{pmatrix} = \begin{pmatrix} \frac{l\sqrt{mgK_F}}{I_{xx}}(\delta\omega_2^2 - \delta\omega_4^2) \\ \frac{l\sqrt{mgK_F}}{I_{yy}}(\delta\omega_3^2 - \delta\omega_1^2) \\ \frac{K_M\sqrt{mgK_F}}{I_{zz}}(\delta\omega_1^2 - \delta\omega_2^2 + \delta\omega_3^2 - \delta\omega_4^2) \end{pmatrix} \quad (30)$$

Furthermore, to equate aircraft orientation to the PD controller, where all constants can be chosen based on desired eigenvalues locations,  $\delta\phi = \phi - \phi_C$  and  $\delta\theta = \theta - \theta_C$  where  $\phi_C$  and  $\theta_C$  are commanded roll and pitch values

$$\begin{pmatrix} \delta\omega_2 - \delta\omega_4 \\ \delta\omega_3 - \delta\omega_1 \\ \delta\omega_1 - \delta\omega_2 + \delta\omega_3 - \delta\omega_4 \end{pmatrix} = \begin{pmatrix} -k_\phi^v \dot{\phi} - k_\phi^p \phi \\ -k_\theta^v \dot{\theta} - k_\theta^p \theta \\ -k_\psi^v \dot{\psi} - k_\psi^p \psi \end{pmatrix} = \begin{pmatrix} \delta\omega_\phi \\ \delta\omega_\theta \\ \delta\omega_\psi \end{pmatrix}$$

Moreover, in order to determine the variation in rotor speeds  $\delta\omega_i$  for all  $i$ , we can impose that  $\delta\omega_z = \delta\omega_1 + \delta\omega_2 + \delta\omega_3 + \delta\omega_4$  being proportional to the variation of the total thrust

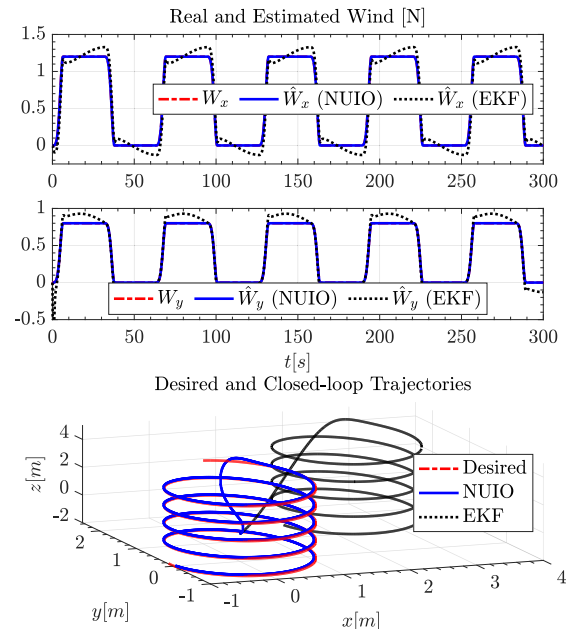


**FIGURE 7. Scenario #2 (Matlab simulation) - Results of wind estimation for time-varying wind gusts and desired and closed-loop spiral trajectories in 3D space. The NUIO-based estimation and control scheme achieves accurate tracking of the desired trajectory, while the EKF-based one shows a large error due to less prompt and accurate wind gust estimation.**

for cross configuration quadrotor gives

$$\begin{pmatrix} 1 & 1 & 1 & 1 \\ 0 & 1 & 0 & -1 \\ -1 & 0 & 1 & 0 \\ 0 & -1 & 1 & -1 \end{pmatrix} \begin{pmatrix} \delta\omega_1 \\ \delta\omega_2 \\ \delta\omega_3 \\ \delta\omega_4 \end{pmatrix} = \begin{pmatrix} \delta\omega_z \\ \delta\omega_\phi \\ \delta\omega_\theta \\ \delta\omega_\psi \end{pmatrix},$$

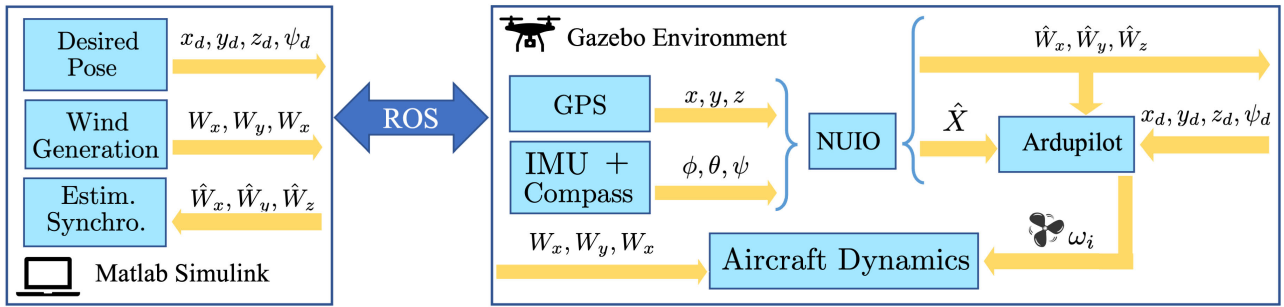


**FIGURE 8.** Data-flow in the ROS Gazebo setup in the Gazebo and the MATLAB/Simulink. ROS nodes and topics are represented by blocks and arrows, respectively. The desired pose and the unknown wind signal are generated in Matlab/Simulink and continuously sent to Gazebo via ROS. The wind signal is used in Gazebo, along with the signal of the robot speeds to simulate the nonlinear aircraft model. Gazebo environment includes GPS, IMU, and compass sensors to emulate the outputs of the aircraft. A ROS-based UIO node is present in Gazebo which reconstructs the unknown wind signal. This information as well as that of the estimated aircraft state and desired pose is used by the Ardupilot controller to generate the rotor speeds.

**TABLE 1.** Erlecopter’s parameters.

Parameter	Value	Description
$m$	1.12 Kg	Total mass
$I_{xx}$	$3.48 \cdot 10^{-2}$ Kg·m <sup>2</sup>	Inertia along $x$
$I_{yy}$	$4.59 \cdot 10^{-2}$ Kg·m <sup>2</sup>	Inertia along $y$
$I_{zz}$	$9.77 \cdot 10^{-2}$ Kg·m <sup>2</sup>	Inertia along $z$
$k_F$	$8.55 \cdot 10^{-2}$ N·m/rad <sup>2</sup>	drag constant
$k_M$	$1.60 \cdot 10^{-2}$ N·m/rad <sup>2</sup>	thrust constant
$l$	0.141 m	axle length

which then gives

$$\begin{pmatrix} \delta\omega_1 \\ \delta\omega_2 \\ \delta\omega_3 \\ \delta\omega_4 \end{pmatrix} = \frac{1}{4} \begin{pmatrix} 1 & 0 & -2 & 1 \\ 1 & 2 & 0 & -1 \\ 1 & 0 & 2 & 1 \\ 1 & -2 & 0 & -1 \end{pmatrix} \begin{pmatrix} \delta\omega_z \\ \delta\omega_\phi \\ \delta\omega_\theta \\ \delta\omega_\psi \end{pmatrix}.$$

Putting everything together in the original coordinate frame, the linear feedback attitude controller which corrects the rotor speeds after estimating wind gusts. Fig. 5 shows the attitude and position controller feeding rotor speeds to quadrotor.

$$\begin{pmatrix} \omega_1 \\ \omega_2 \\ \omega_3 \\ \omega_4 \end{pmatrix} = \frac{\begin{pmatrix} \frac{1}{4} & 0 & \frac{I_{yy}}{2l} & -\frac{I_{zz}}{K_M} \\ \frac{1}{4} & -\frac{I_{xx}}{2l} & 0 & \frac{I_{zz}}{K_M} \\ \frac{1}{4} & 0 & \frac{I_{yy}}{2l} & -\frac{I_{zz}}{K_M} \\ \frac{1}{4} & \frac{I_{xx}}{2l} & 0 & \frac{I_{zz}}{K_M} \end{pmatrix}}{\sqrt{mgK_F}} \begin{pmatrix} 2mg + \sqrt{mgK_F}\delta\omega_z \\ k_\phi^v \dot{\phi} + k_\phi^p (\phi - \phi_C) \\ k_\theta^v \dot{\theta} + k_\theta^p (\theta - \theta_C) \\ k_\psi^v \dot{\psi} + k_\psi^p (\psi - \psi_d) \end{pmatrix}. \quad (31)$$

Finally, Fig. 6 and 7 show the robustness of the proposed NUIO in simulation when exposed to military grade and time varying wind gusts for circular and helical trajectory of the nonlinear model of quadrotor aircraft. Results obtained when using an EKF are also reported in the figures for comparison purposes. It is worthy noticing that the proposed NUIO can work with any type of controller, provided that the controller itself can compensate for the estimated wind gusts by changing the rotor speeds.

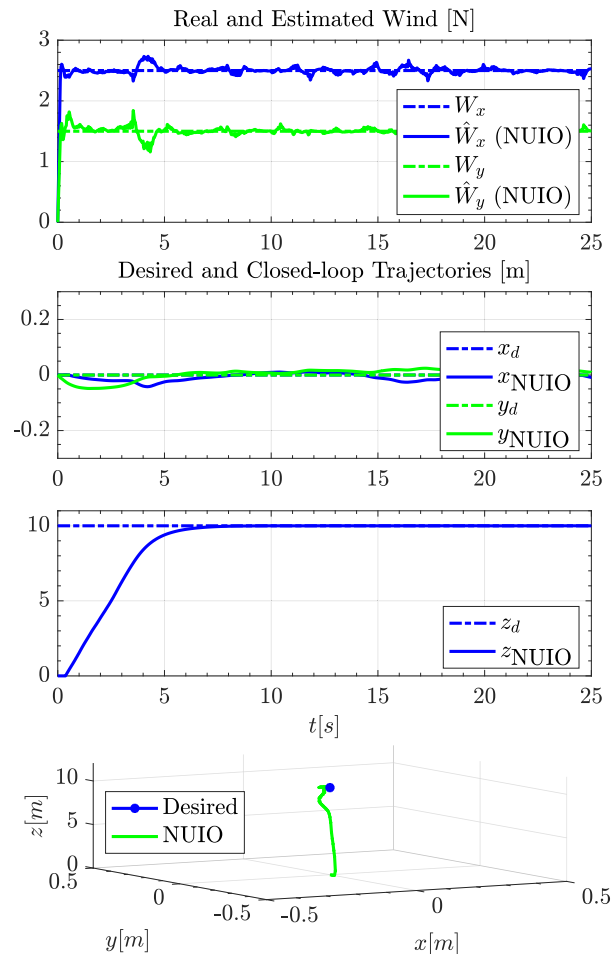


**FIGURE 9.** Scenario #1 (Gazebo simulation) - From top to down, results showing the estimated wind, desired and closed-loop trajectories and 3D representation.

## V. SIMULATION AND ROS GAZEBO VALIDATION

The parameters of the Erlecopter [39] prototype aircraft have been used to carry out the Matlab/Simulink and ROS/Gazebo simulation and are the same as those shown in Table 1.

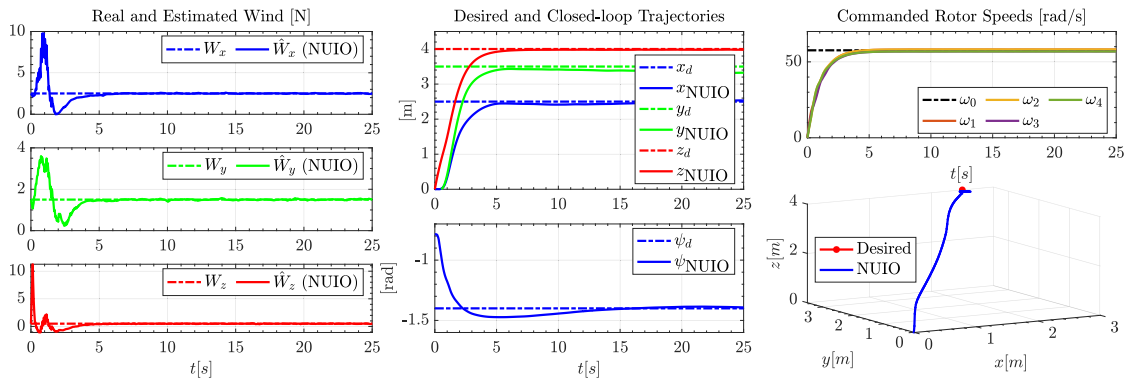


**FIGURE 10. Scenario #2 (Gazebo simulation) - Results of step wind gusts showing wind gust estimation (left), middle section shows the quadrotors positions; top right figure shows the rotor speeds and the 3D trajectory is on bottom right.**

### A. SIMULINK VALIDATION

The first step of validation is to use the proposed scheme in the Matlab/Simulink environment. The nonlinear mathematical model of the quadrotor together with the wind estimation scheme of the NUIO have been implemented. The system parameters are the same as discussed in Table 1. The control system has been tested under two different scenarios: 1) military gusts winds affecting the aircraft when it is required to tracking a circular trajectory, and 2) time-varying wind spiral trajectory of the quadrotor.

#### 1) SCENARIO #1

As a first validation step, the quadrotor is required to move along a circular trajectory of radius 5 m at a height  $z_d = 5$  m, in the presence of military-grade type wind gusts [40]. The controller's parameters are chosen as  $k_x^p = k_y^p = k_z^p = k_p^\phi = k_\theta^p = k_\psi^p = 0.9$  and  $k_x^v = k_y^v = k_z^v = k_\phi^v = k_\theta^v = k_\psi^v = 9$ , so that the quadrotor can accurately and smoothly track the desired trajectory and the yaw variable  $\psi$  is can converge to zero within 10 s. Simulation results presented in Fig. 6 shows the NUIO correctly estimates the wind gusts with a very small error also during the initial transient. The dotted line shows the desired and the solid line shows the estimated wind, the EKF is illustrated in black for comparison.

#### 2) SCENARIO #2

The Matlab simulation design is also tested for a large time-varying wind gust as shown in Fig. 7. The quadrotor is required to move at a height  $z_d = 4$  m and then land in a spiral path in the presence of time-varying wind gust. The control parameters are chosen as in Scenario #1, again with the aim to let the quadrotor reach the desired path more accurately and smoothly.

### B. ROS/GAZEBO VALIDATION

The proposed design is then tested within the ROS/Gazebo framework using Ardupilot 3.5 controller. The Ardupilot has its own nonlinear controller, which proves that the NUIO proposed works for any type of controller, provided the rotor

speeds and partial outputs are available to the NUIO for estimation of wind gusts. The ROS nodes communicate to the Simulink and Gazebo software.

Fig. 8 shows the communication links between Gazebo, ROS, and Ardupilot. Gazebo is designed to accurately reproduce the dynamic environment of a quadrotor [39]. The simulated prototype has mass, inertia, wind, friction, and numerous other attributes that allow it to behave realistically when testing. These actions are also integral parts of an experiment. The aircraft prototype has been developed by Erle Robotics for Gazebo, and it has a dynamic structure composed of a rigid body with joints, forces, and torques to generate propulsion and interaction with the environment. More precisely, the architecture implemented is as follows:

- 1) ROS provides a middleware layer for the SITL (software in the loop) emulation,
- 2) the Gazebo software provides a reliable simulation platform for the aircraft physics, including wind gust forces, and
- 3) Matlab/Simulink scheme implements the proposed NUIO filter. Gazebo receives rotor speeds from subscribed ROS topics and publishes the aircraft pose (position and attitude) to ROS, while the Matlab/Simulink node subscribes and receives such pose topics.

#### 1) SCENARIO #1

The proposed NUIO is tested with a constant horizontal wind gusts of  $W_x = 1.2$  N and  $W_y = 2.4$  N. The quadrotor is required to hover at the height of  $z_d = 10$  m while  $\psi$  is determined by the Ardupilot to the value  $-0.5$  rad. Results of the simulation are reported in Fig. 9.

#### 2) SCENARIO #2

The NUIO is tested with constant wind gusts of  $W_x = 2.5$  N,  $W_y = 1.5$  N and  $W_z = 0.5$  N. The quadrotor is required to move from the origin to  $x_d = 2.5$  m,  $y_d = 3.5$  m and  $z_d = 4$  m along a straight line and  $\psi$  is determined by the Ardupilot as  $-1.4$  rad. In the Gazebo environment the  $\omega_0$

is 57.7 rad/s, but the quadrotor rotor speeds are 55 rad/s, less than  $\omega_0$  due to the wind gust acting along the positive  $z$  direction pushing the quadrotor. The wind speed vector components,  $v_x$  and  $v_y$ , are easily obtained from wind force components,  $W_x$  and  $W_y$ , by using the conversion formula  $W_i = \rho S_x v_i^2$ , for  $i \in \{x, y\}$ , where  $\rho = 1.225 \text{ kg/m}^3$  is the air density at sea level and quadrotor lateral sections, which, for small roll and pitch, can be approximated to  $S_x = S_y = 9.88 \times 10^{-3} \text{ m}^2$ .

## VI. CONCLUSION

To conclude, the paper presents an innovative approach to accurately estimate and compensate the external disturbances in real-time such as wind gusts acting on the nonlinear model of the quadrotor aircraft. The quadrotor has robust performance as it moves accurately along the desired path when exposed to different types of wind gusts which is validated by Matlab/Simulink and Gazebo environment. This shows that the proposed method requires no extra sensors, is simple low computation and has the ability to obtain a fast respond to different types of disturbances during the flight. Furthermore, the nonlinear unknown input observer works with any type of controller, provided the controller can compensate for the estimated wind gusts by changing the aircraft rotor speed. This has been proved as for simulation by using PD controller and in Gazebo environment using Ardupilot controller. The performance of the controller is obviously affected by the parameters of the controller (PD), thus an accurate design is requested. Nevertheless, the parameters of the NUIO only depend on the model parameters. Future work will focus on on-line model parameter estimation, to make the NUIO adaptive. Another possible approach that can handle parameter uncertainty is the adoption of back-stepping techniques. Finally, this independent type of robust control method has multiple real world applications such as flying the quadrotor accurately and independently in windy conditions.

## REFERENCES

- [1] R. Miranda-Colorado and L. T. Aguilar, "Robust PID control of quadrotors with power reduction analysis," *ISA Trans.*, vol. 98, pp. 47–62, Mar. 2020.
- [2] V. M. Babu, K. Das, and S. Kumar, "Designing of self tuning PID controller for AR drone quadrotor," in *Proc. 18th Int. Conf. Adv. Robot. (ICAR)*, 2017, pp. 167–172, doi: [10.1109/ICAR.2017.8023513](https://doi.org/10.1109/ICAR.2017.8023513).
- [3] F. Santoso, M. A. Garratt, and S. G. Anavatti, "Hybrid PD-fuzzy and PD controllers for trajectory tracking of a quadrotor unmanned aerial vehicle: Autopilot designs and real-time flight tests," *IEEE Trans. Syst., Man, Cybern., Syst.*, vol. 51, no. 3, pp. 1817–1829, Apr. 2021.
- [4] F. Sabatino, "Quadrotor control: Modeling, nonlinear control design, and simulation," M.S. thesis, School Elect. Eng. Comput. Sci., KTH Roy. Inst. Technol., Stockholm, Sweden, 2015.
- [5] R. Falcón, H. Ríos, and A. Dzul, "Comparative analysis of continuous sliding-modes control strategies for quad-rotor robust tracking," *Control Eng. Pract.*, vol. 90, pp. 241–256, Sep. 2019.
- [6] M. Bhargavapuri, S. R. Sahoo, M. Kothari, and Abhishek, "Robust nonlinear control of a variable-pitch quadrotor with the flip maneuver," *Control Eng. Pract.*, vol. 87, pp. 26–42, Jun. 2019.
- [7] D. Lee, H. J. Kim, and S. Sastry, "Feedback linearization vs. adaptive sliding mode control for a quadrotor helicopter," *Int. J. Control, Autom., Syst.*, vol. 7, no. 3, pp. 419–428, Jun. 2009.
- [8] E. Sariyildiz, R. Oboe, and K. Ohnishi, "Disturbance observer-based robust control and its applications: 35th anniversary overview," *IEEE Trans. Ind. Electron.*, vol. 67, no. 3, pp. 2042–2053, Mar. 2020.
- [9] G. Hostetter and J. S. Meditch, "Observing systems with unmeasurable inputs," *IEEE Trans. Autom. Control*, vol. AC-18, no. 3, pp. 307–308, Jun. 1973.
- [10] S.-H. Wang, E. Wang, and P. Dorato, "Observing the states of systems with unmeasurable disturbances," *IEEE Trans. Autom. Control*, vol. AC-20, no. 5, pp. 716–717, Oct. 1975.
- [11] P. Kudva, N. Viswanadham, and A. Ramakrishna, "Observers for linear systems with unknown inputs," *IEEE Trans. Autom. Control*, vol. AC-25, no. 1, pp. 113–115, Feb. 1980.
- [12] S. P. Bhattacharyya, "Observer design for linear systems with unknown inputs," *IEEE Trans. Autom. Control*, vol. AC-23, no. 3, pp. 483–484, Jun. 1978.
- [13] R. J. Miller and R. Mukundan, "On designing reduced-order observers for linear time-invariant systems subject to unknown inputs," *Int. J. Control*, vol. 35, no. 1, pp. 183–188, Jan. 1982.
- [14] N. Kobayashi and T. Nakamizo, "An observer design for linear systems with unknown inputs," *Int. J. Control*, vol. 35, no. 4, pp. 605–619, Apr. 1982.
- [15] A. H. Al-Bayati, Z. Skaf, and H. Wang, "A comparative study of nonlinear observers applied to a DC servo motor," in *Proc. 8th World Congr. Intell. Control Autom.*, Jul. 2010, pp. 785–790.
- [16] F. Yang and R. W. Wilde, "Observers for linear systems with unknown inputs," *IEEE Trans. Autom. Control*, vol. 33, no. 7, pp. 677–681, Jul. 1988.
- [17] S. Li, J. Yang, W.-H. Chen, and X. Chen, *Disturbance Observer-Based Control: Methods and Applications*, 1st ed. Boca Raton, FL, USA: CRC Press, 2014.
- [18] K. T. Borup, B. N. Stovner, T. I. Fossen, and T. A. Johansen, "Kalman filters for air data system bias correction for a fixed-wing UAV," *IEEE Trans. Control Syst. Technol.*, vol. 28, no. 6, pp. 2164–2176, Nov. 2020.
- [19] W. Song, "An integrated GPS/vision UAV navigation system based on Kalman filter," in *Proc. IEEE Int. Conf. Artif. Intell. Inf. Syst. (ICAIS)*, Mar. 2020, pp. 376–380.
- [20] A. Shastry and D. A. Paley, "UAV state and parameter estimation in wind using calibration trajectories optimized for observability," *IEEE Control Syst. Lett.*, vol. 5, no. 5, pp. 1801–1806, Nov. 2021.
- [21] P. Taylor, N. Kobayashi, and T. Nakamizo, "An observer design for linear systems with unknown inputs," *Int. J. Control*, vol. 35, no. 4, pp. 37–41, 2007.
- [22] S. Sundaram and C. N. H. C. N. Hadjicostis, "Delayed observers for linear systems with unknown inputs," *IEEE Trans. Autom. Control*, vol. 52, no. 2, pp. 384–387, Feb. 2007.
- [23] A. Gonzalez, V. Balaguer, P. Garcia, and A. Cuenca, "Gain-scheduled predictive extended state observer for time-varying delays systems with mismatched disturbances," *ISA Trans.*, vol. 84, pp. 206–213, Jan. 2019.
- [24] R. Rajamani and Y. M. Cho, "Existence and design of observers for nonlinear systems: Relation to distance to unobservability," *Int. J. Control*, vol. 69, no. 5, pp. 717–731, 1998.
- [25] M. Witczak and P. Pretki, "Design of an extended unknown input observer with stochastic robustness techniques and evolutionary algorithms," *Int. J. Control*, vol. 80, no. 5, pp. 749–762, May 2007.
- [26] B. W. Seifeddine, D. Slim, and B. H. Fayçal, "Unknown inputs observers for state and unknown inputs estimation in a class of discrete-time Lipschitz nonlinear systems," in *Proc. Int. Conf. Elect. Eng. Softw. Appl.*, 2013, pp. 1–5, doi: [10.1109/ICEESA.2013.6578384](https://doi.org/10.1109/ICEESA.2013.6578384).
- [27] V. Sharma, V. Agrawal, B. B. Sharma, and R. Nath, "Unknown input nonlinear observer design for continuous and discrete time systems with input recovery scheme," *Nonlinear Dyn.*, vol. 85, no. 1, pp. 645–658, Jul. 2016.
- [28] S. I. Abdelmaksoud, M. Mailah, and A. M. Abdallah, "Robust intelligent self-tuning active force control of a quadrotor with improved body jerk performance," *IEEE Access*, vol. 8, pp. 150037–150050, 2020.
- [29] D. J. Almkhles, "Robust backstepping sliding mode control for a quadrotor trajectory tracking application," *IEEE Access*, vol. 8, pp. 5515–5525, 2020.
- [30] L. Liu, W. X. Zheng, and S. Ding, "An adaptive SOSM controller design by using a sliding-mode-based filter and its application to buck converter," *IEEE Trans. Circuits Syst. I, Reg. Papers*, vol. 67, no. 7, pp. 2409–2418, Jul. 2020.
- [31] L. Liu, S. Ding, and X. Yu, "Second-order sliding mode control design subject to an asymmetric output constraint," *IEEE Trans. Circuits Syst. II, Exp. Briefs*, vol. 68, no. 4, pp. 1278–1282, Apr. 2021.

- [32] W. Zhao, H. Liu, F. L. Lewis, K. P. Valavanis, and X. Wang, "Robust visual servoing control for ground target tracking of quadrotors," *IEEE Trans. Control Syst. Technol.*, vol. 28, no. 5, pp. 1980–1987, Sep. 2020.
- [33] H. A. Hashim, "Guaranteed performance nonlinear observer for simultaneous localization and mapping," *IEEE Control Syst. Lett.*, vol. 5, no. 1, pp. 91–96, Jan. 2021.
- [34] X.-L. Ren, "Observer design for actuator failure of a quadrotor," *IEEE Access*, vol. 8, pp. 152742–152750, 2020.
- [35] T. Yang, N. Sun, and Y. Fang, "Adaptive fuzzy control for a class of MIMO underactuated systems with plant uncertainties and actuator deadzones: Design and experiments," *IEEE Trans. Cybern.*, early access, Feb. 2, 2021, doi: 10.1109/TCYB.2021.3050475.
- [36] A. Castillo, R. Sanz, P. Garcia, W. Qiu, H. Wang, and C. Xu, "Disturbance observer-based quadrotor attitude tracking control for aggressive maneuvers," *Control Eng. Pract.*, vol. 82, pp. 14–23, Jan. 2019.
- [37] E. Sariyildiz, R. Mutlu, and C. Zhang, "Active disturbance rejection based robust trajectory tracking controller design in state space," *ASME. J. Dyn. Syst., Meas., Control*, vol. 141, no. 6, Jun. 2019.
- [38] E. Sariyildiz and K. Ohnishi, "Analysis the robustness of control systems based on disturbance observer," *Int. J. Control*, vol. 86, no. 10, pp. 1733–1743, 2013.
- [39] K. Kumar, S. I. Azid, A. Fagiolini, and M. Cirrincione, "Erle-copter simulation using ROS and gazebo," in *Proc. IEEE 20th Medit. Electrotech. Conf. (MELECON)*, Jun. 2020, pp. 259–263.
- [40] MATLAB. (2020). *Discrete Wind Gust Model*. [Online]. Available: <https://www.mathworks.com/help/aeroblks/discretewindgustmodel.html>



**KRISHNEEL KUMAR** received the Bachelor of Engineering degree in electrical and electronics, in 2017, and the Master of Science degree in engineering in the field of robotics and control from The University of the South Pacific, in 2019. He is currently pursuing the Ph.D. degree in science and technologies for electrical engineering and complex systems for mobility with the University of Genova, Italy. He was awarded a Gold Medal for the Bachelor of Engineering degree.



**MAURIZIO CIRRINCIONE** (Senior Member, IEEE) received the Laurea degree in electrical engineering from the Politecnico di Torino, Italy, in 1991, and the Ph.D. degree in electrical engineering from the University of Palermo, Italy, in 1996. From 1996 to 2005, he was a Researcher with the ISSIA-CNR (Institute on Intelligent Systems for Automation), Palermo. Since 2005, he has been a Full Professor of control systems at the UTBM, Belfort, France, and a member of the IRTES Laboratory and the Fuel Cell Laboratory (FCLaboratory), Belfort. Since April 2014, he has been the Head of the School of Engineering and Physics, The University of the South Pacific, Suva, Fiji. Since 2016, he has been a 1st Class Full Professor. He is the author of over 155 articles, 55 of which on high-impact factor journals, and of two books. He was awarded the 1997 "E. R. Caianiello" prize in 1997 for the Best Italian Ph.D. thesis on neural networks.



**SHEIKH IZZAL AZID** (Member, IEEE) received the M.Sc. degree in engineering in the area of automation and intelligent systems, in 2010, and the Ph.D. degree in the area of aerial robotics and robust control from The University of the South Pacific in collaboration with the University of Palermo, Italy. He is currently a Lecturer with the School of Engineering and Physics, The University of the South Pacific. He also worked as a Consultant for several European Projects on Science,

Technology, and Innovation in the Pacific. His research interests include robotics, controls, autonomous systems, state observers, and microprocessor applications. He was a recipient of the Erasmus+ staff exchange program and he was attached at the Technical University of Sofia. He is the Vice President of IEEE VTS New Zealand North.



**ADRIANO FAGIOLINI** (Member, IEEE) received the M.S. degree in computer science engineering and the Ph.D. degree in robotics and automation from the University of Pisa, in 2004 and 2009, respectively. He has been a Visiting Researcher with the Department of Energy, IUT Longwy Université de Lorraine, France, in 2019, and at the Department of Mechanical Engineering, University of California at Riverside, in 2015 and 2017.

He enrolled in the Summer Student Program at the European Center for Nuclear Research (CERN), Geneva, in 2002. In 2008, he led the Team of the University of Pisa during the first European Space Agency's Lunar Robotics Challenge, which resulted in a second-place prize for the team. He is currently an Assistant Professor with the University of Palermo, Italy. He was one of the recipients of the IEEE ICRA Best Manipulation Paper Award in 2005.

...